RSC Advances

ROYAL SOCIETY OF CHEMISTRY

www.rsc.org/advances

On the Large Capacitance of Nitrogen Doped Graphene Derived by a Facile Route

M. Praveen Kumar[1], T. Kesavan[1], Golap Kalita[2],
P. Ragupathy[1,*], Tharangattu N. Narayanan[1] and Deepak K. Pattanayak[1,*]

[1]CSIR - Central Electrochemical Research Institute, Karaikudi-630006, India.
[2]Nagoya Institute of Technology, Gokisho-cho, Nagoya-4668555, Japan.

* Corresponding Authors.
E-mail: (D. K. P) deepak@cecri.res.in: (P. R) ragupathyp@cecri.res.in

Abstract

Recent research activities on graphene identified doping of foreign atoms in to the honeycomb lattice as a facile route to tailor its bandgap. Moreover, the presence of foreign atoms can acts as defective centres in basal plane, and these centres can enhance the electrochemical activities of graphene surface. Here, we report a facile synthesis approach for the bulk synthesis of nitrogen doped graphene (N- Graphene) from graphene oxide by a hydrothermal process, with a large control over the amount of N-doping. The electrochemical activeness of N- Graphene (with 4.5 atomic % of nitrogen) is studied by conducting supercapacitor measurements. The N- Graphene exhibits remarkably high specific capacitance of 459 Fg^{-1}at a current density of 1 mA in 1 M H_2SO_4 electrolyte with a high cycle stability compared to that of pristine graphene having a specific capacitance of 190 Fg^{-1}. The structure destabilisation of graphene in higher pH / high amount alkaline treatment is demonstrated, and hence optimization of amount reagents is necessary in developing graphene based high performance electronic or electrochemical devices.

Keywords: Nitrogen doping: Supercapacitor: Graphene: Defects: Foreign atoms: EDLC: Alkaline reduction: Structure destabilisation.

1. Introduction

Development of high power and energy density supercapacitors (SCs) has become one of the prime research areas in recent energy technology.[1, 2] Based on the mode of charge energy storage mechanism, SCs are broadly classified into two categories (i) double layer capacitance (Electric Double Layer Capacitance (EDLC)) in which charge is stored between electrode / electrolyte interfaces, while (ii) faradaic process is responsible for charge storage in supercapacitors. However, the energy density of SCs (30 $WhKg^{-1}$) is significantly lower than that of batteries (200 $WhKg^{-1}$) and fuel cells. Relatively low specific capacitance of EDLC, in the range of 100-300 Fg^{-1} in aqueous electrolyte and 100-150 Fg^{-1} in non aqueous electrolytes, is not able to satisfy the energy demand of many applications.[3] Thus, it is of great interest to build SCs from new materials with low cost, high capacitance and excellent cyclability. Out of various materials used for SC applications, carbon based materials place a unique role due to the availability of various crystalline forms of carbon with relatively high conductivity and surface area.

Graphene, a 2-dimensional (2D) carbon nanostructure, has attracted great interest for applications in the fields of energy storage and conversion because of its unique physicochemical properties such as high surface area, excellent conductivity and mechanical strength. However, the reported capacitance values for graphene based SCs are much inferior to the theoretical capacitance of single layer graphene.[4] This can be due to the unavoidable curling and bundling of graphene during the device fabrication, resulting in to a large reduction of its active surface area. Hence, improving the capacitance of graphene materials is of great interest, many attempts have been underwent, including the introduction of dopants, and development of graphene / metal / metal oxides hybrids.[5-9]

Doping foreign elements such as nitrogen (N) is accepted as a simple and effective way to tailor the local electronic structure of graphene,[10, 11] and because of its atomic size and strong valence bonds similar to those of carbon atoms, nitrogen can be doped into the lattice of graphene – retaining its sp^2 functionalization, particularly N- doped graphene (N-Graphene) synthesized at very high temperatures (above 900°C) will give quaternary nitrogen.[12] It has been widely accepted that the manipulated local electronic structure enhance the binding phenomenon with ions,[13] and hence this feature can be utilized for making high performance storage devices from doped graphene.[14] To the date, various methods have been reported for the synthesis of N-Graphene including chemical vapour deposition (CVD),[15] nitrogen plasma process,[16] electrochemical reactions,[17] thermal annealing with urea,[18] and solvothermal route.[19] However, vigorous reaction conditions and sophisticated instruments are the main obstacles to scale up the process and increase the N- content. On the other hand, hydrothermal methods along with reagents such as amine,[20] pyrrole,[21] urea,[22] and hexamethylenetetramine[23] as the nitrogen sources have the advantage of mild reaction and easy to prepare in a large quantity of N- Graphene. Reported capacitance values for N-Graphene based SCs lie only in the range of 150 - 370 Fg^{-1} (please see Table 1). Thus, it is necessary to further increase the specific capacitance of N- Graphene by controlled nitrogen doping, if possible.

Here, we report a very simple and low cost approach for the synthesis of N- Graphene by a hydrothermal technique using ammonium hydroxide as nitrogen source, in the presence of hydrazine hydrate as a reducing agent. The electrochemical performance of N- Graphene is investigated by cyclic voltammetry (CV) and galvanostatic charge-discharge cycling. The influence of nitrogen doping on graphene and its electrochemical performance are systematically correlated and reported.

2. Experimental section

2.1. Synthesis of N-doped graphene

Graphene Oxide (GO) has been synthesized by following the "Improved Method" reported by Tour et al for the synthesis of high quality GO from graphite powder.[24] In this method, Graphite (2 g) is thoroughly mixed with the mixture of sulfuric acid and phosphoric acid (9 : 1 ratio) (Alfa aesar) at room temperature by magnetic stirring. Potassium permanganate (14 g) crystals are then slowly added to this mixture. The resultant mixture is stirred well by keeping the temperature at 90°C for 24 hrs. Then, 14 mL of 30 % H_2O_2 (Alfa aesar) is added to this mixture, after keeping the mixture in an ice bath. The solution was subjected to vacuum filtration, and the residue was washed with water, 5 % HCl and ethanol subsequently for 3 cycles. The resultant filtrate (GO) is soaked in ether and dried in a vacuum oven at 80°C for 24 hrs.

The GO (0.1 g) is dispersed in deionised water (93 mL), and 7 mL of hydrazine hydrate (N_2H_4) is added to this GO solution with a continuous stirring. After 2 hrs, ammonium hydroxide is added to this mixture (volume of ammonium hydroxide is varied from 3 - 10 mL in different samples to get different level of doping) and the mixture solution is kept in a teflon autoclave. Autoclave is kept in an oven at 180°C for 12 hrs. The residue is collected and dispersed in water and vacuum filtrated using a PTFE membrane filter paper (pore size = 0.22 μm). This residue is washed several times with DI water to make the pH ~ 7. The filtrate is collected and allowed to dry at 50°C for 24 hrs in an oven. The resultant powder is collected and used for the further experiments.

2.2. Physiochemical characterization:

The structure, morphology and texture were characterized by powder X-ray diffraction (XRD), Field emission scanning electron microscopy (FE-SEM) and transmission electron microscopy (TEM). In order to confirm the crystal structure and phase purity of the

sample, powder X-ray diffraction patterns were recorded on a Bruker D 8 Advance X-ray diffractometer with Cu Kα (λ = 1.5405 Å) radiation in the range of 5-65º (2θ). Raman measurements were carried out using Renishaw (UK) In Via Raman microscope with 632.8 nm wavelength incident laser light. The morphology and structural properties of the as-synthesized graphene and N- Graphene were investigated using a FE-SEM (Carl Zesis, SUPRA 55VPFEI, Germany).TEM images of samples were taken using a FEI TECNAI $G^2$20 with an accelerating voltage of 200 kV. TEM samples were prepared (mixing DMF and sample under sonication for 45 min) by placing a drop of solution on a carbon-coated copper grid and drying under UV light. Presence of functional groups in graphene as well as N-Graphene were observed using FTIR (BRUKER OPTIK GMBH, Germany; Model no TENSOR 27). X-ray photoelectron spectroscopy (XPS) was carried out with PHI 5000 VersaProbe ULVAC instrument. A Schimadzu balance of model 220D with 10 mg sensitivity was used for weighing the materials.

2.3. Electrode preparation and electrochemical characterization:

High-purity stainless steel foil was polished with successive grades of emery paper, cleaned with detergent, washed with double distilled water, rinsed with acetone and dried in air. The foil was slurry-coated with 75 wt. % N- Graphene, 20 wt. % Super P and 5 wt. % PVDF in NMP, and dried at 100 °C under vacuum for 12 hrs (area of coating:1 cm^{-2}). Electrochemical studies were carried out using a (PARSTAT 4000, Princeton Applied Research, AMETEK private Ltd., Pune, India.) in a three-electrode configuration with N-Graphene as the working electrode, Pt as the counter electrode and a saturated calomel electrode (SCE) as the reference electrode. 1 M H_2SO_4 was used as an electrolyte. Discharge specific capacitance (SC) of N- Graphene was calculated using the formula

$$SC = It/m\Delta E \qquad 1$$

Where, I is current in amps used for charge / discharge cycling, t is the time in seconds of discharge, m is the mass in grams of the active material and ΔE is the operating potential window in volt of charge or discharge.

3. Results and discussion

Figure 1 shows powder XRD pattern for graphite, GO, graphene and N- Graphene prepared in different volume of ammonium hydroxide. The (002) plane of graphite is clearly seen at a 2θ of 26.54°(JCPDS # 656212) with interlayer spacing (d value) of 0.33 nm, while that of GO is shifted from 26.54° to 11.07° indicating the increase in 'd' value from 0.33 nm to 0.79 nm due to the complete oxidation and exfoliation of graphite. This is in tune with the earlier reports.[25] The interlayer spacing of graphene (graphene synthesized by this route) and N- Graphene are larger than that of graphite.[26] The chemically reduced GO (graphene) possessed a broad peak catered at 23.87° with a corresponding d- spacing of ~ 0.37 nm. However, hydrothermally synthesized N- Graphene with varying ammonium hydroxide (3 to 10 mL) showed pronounced peaks at 24.22, 25.94, 25.7 and 25.7° with corresponding interlayer spacing of 0.36, 0.34, 0.34 and 0.34 nm, respectively. The 3 mL sample showed highest crystallinity among all the doped samples. The interlayer spacing was little decreased near to graphite atomic layer (0.33 nm) with increasing amount of ammonium hydroxide i.e. from 3 to 10 mL, probably due to the further reduction of RGO. Moreover, it is also noticed that increasing the amount of ammonium hydroxide is also broadened the graphitic peak corresponding to (002) plane, indicating the lowering of crystallinity, and this is in tune with the earlier reports.[27]

Figure 2 shows the Raman spectra of graphite, graphene oxide and N- Graphene. The two typical peaks in the graphene based materials are observed at 1348 cm^{-1} and 1580 cm^{-1} referred as D and G bands where D band shows the presence of defects in the graphitic lattice

with A1g symmetry, while the latter peak, namely, a G band, is associated with the in-plane E_{2g} mode of single crystalline graphitic carbon atoms in the honeycomb lattice. Generally, I_D / I_G ratio provides the information about in plane crystallite dimension, in plane defects and edge defects and the disorder nature of graphene derivatives. It is well documented that the introduction of N atoms into graphene can enhances the formation of lot of defects resulting a high intensity of D band due to formation of smaller nanocrystalline graphene domains by heteroatom doping.[28, 29] The D and G bands obtained for graphite clearly indicates the absence of disorder. As shown in Figure 2, the significant increase in D band in the N-Graphene clearly indicates the defects and disorder structure of N- Graphene. The increase in I_D / I_G band ratio from 0.95 to 1.10 in the Raman spectra as shown in Figure 2 is an indication of increasing defects on increase of ammonium hydroxide content. The high I_D / I_G ratio of N-Graphene compared to that of pristine graphene clearly demonstrates the large structural defects and edge plane exposure caused by heterogeneous N atoms insertion into the graphene layers. However, there is not much change in the I_D / I_G ratio for various N-Graphene, possibly due to merely similar defects created during different amount of N doping.

Fourier transform infrared (FTIR) spectroscopy is an ideal analytical tool to identify the functional groups present in graphite, intercalation of graphite oxide (GO) by oxidation, graphene and N- Graphene. Figure 3 shows the typical FTIR spectra of graphite oxide and N-Graphene prepared in different ammonium hydroxide content. Two remarkable absorption peaks obtained at 3400 and 1032 cm^{-1} clearly indicates the presence of absorbed water molecules and C-O groups, respectively. The graphite oxide (GO) exhibits a band at 1725 cm^{-1}, which is assigned to the carbonyl (C=O) stretching groups. This stretching is pronounced in graphite oxide (GO) sample due to higher degree of oxidation and the strong

peak C-O epoxy group stretching (C-O-C) at 1917 cm^{-1}, whereas graphite oxide (GO) shows broad C-O stretching bands from 1000 to 1400 cm^{-1}, indicating coexistation of O=C-OH (carboxyl), C-O-C (epoxy), and C-OH (hydroxyl). It is well known that epoxy and hydroxyl groups exhibits both edge and basal planes while carboxyl groups are mainly grafted on the edges of the oxidized graphite.[30] In plane structure of graphite oxide, the peaks at 1571 and 1725 cm^{-1} are evident for C=C and C=O bands. The peaks at 3004 and 3434 cm^{-1} correspond to C-H and O-H groups. The graphite oxide was chemically reduced by hydrazine hydrate reduction process. After reduction reaction, the peak 1725 cm^{-1} corresponds to the weak and sharp C=O stretching groups. The GO has been successfully reduced by hydrazine hydrate to obtain graphene. In N- Graphene, nitrogen atom replaces carbon atom. The peaks appeared at 1187 and 1571cm^{-1} in the N- Graphene correspond to the strong and sharp peak C-N and C=C stretching bond respectively (Figure 3).

FE-SEM images of graphite, graphite oxide (GO), graphene (GN) and N- Graphene are shown in Figure 4. The graphite powder was composed of number of flake like layers (Figure 4a). However, after oxidation process, these graphite layers were exfoliated and subsequently intercalated by epoxy, carboxyl and hydroxyl functional groups. The GN maintained its two dimensional sheet like structures as seen in the FE-SEM image (Figure 4b). The crystalline structure and transparency of the sheets are clearly maintained in N-Graphene 3 mL and N- Graphene 5 mL (Figure 4c and d). Surprisingly, on increase in the amount of ammonium hydroxide solution the morphology of N- Graphene sheets aggregated during the hydrothermal process and is shown in Figure 4e and f.

TEM image of the GO sheet is shown in Figure 5a and the corresponding Selected Area Electron Diffraction (SAED) pattern is shown in Figure 5a1. After reduction, a single transparent sheet of reduced GO (RGO) was observed and is shown in TEM image (Figure

5b) and hexagonal rings directly visualized in SAED pattern, while N- Graphene appeared like a crumpled sheet as observed in Figure 5c. The morphology of N- Graphene was destroyed while increasing the amount of ammonium hydroxide (>3 mL), and the TEM and corresponding SAED (Figures 5d-f) patterns show amorphous nature, indicting the structural distortion.

N- Graphene was prepared using ammonium hydroxide solution in different volume (3-10 mL) by hydrothermal method. XPS studies confirmed the presence of nitrogen doping in graphene sheet and are shown in Figure 6. XPS results show that with increase in the amount of ammonium hydroxide from 3 to 10 mL, amount of N- doping decreased and is shown in Figure 6. Percentage of nitrogen incorporated into graphene sheet was found to be highest i.e. 4.5 atomic % for 3 mL ammonium hydroxide solution and it decreased to 0.9 to 3.0 atomic % when the amount of ammonium hydroxide increased as shown in Table 2. The increase in pH as seen in Table 2 indicates that the high alkaline environment is not advantageous for nitrogen content.[31, 32] Figure 6a shows the survey scan of N- Graphene (3 mL) and it can be seen that peaks observed at 284.7, 401 and 532.5 eV corresponding to C1s, N1s and O1s, respectively. High resolution of N1s scanning spectrum was deconvoluted into four individual components that pyridinic like N, pyrrolic like N, graphitic like N and pyridinic oxide like N as observed at 399.3, 400.1, 401 and 402.2 and 403 eV, respectively (Figure 6 (ii)). Figure 6 (i) shows the high resolution C1s of 3 mL N-doped graphene after deconvolution into three components, namely, C-N, C-O and C=O corresponding to the peaks observed at 285.9, 286.9 and 288.7 eV, respectively. Electrochemical performance depends on the edge defect on the graphene sheet, like the presence of pyridinic N-Graphene.[33] Here, the percentage of pyridinic N was very low compared to that of pyrrolic and graphitic N. However, high specific capacitance obtained in the present study is possibly

due to the presence of various N- functionalities. The electrocatalytic activity of N- Graphene was found to be dependent on the graphitic N- content, which determines the limiting current density,[34] while pyridinic N contributes to the major part of capacitance increment in N-Graphene among various N- configurations.[35] Further, increasing the volume of ammonium hydroxide leads to the change in microstructure (interplanar spacing due to reduction) as well as crystallinity of the graphene (affect adversely as it is seen from the TEM and SAED studies) which also affect the electrochemical performance of the N- Graphene. The limiting current density proceed the maximum current density to achieve a desired electrode reaction before hydrogen or other extraneous ions are discharged simultaneously and also without undue interference such as from polarization. The high resolution of O1s was obtained at 532 eV (Figure 6(iii)).

Cyclic voltammetry (CV) and galvanostatic charge/discharge are well recognized to be ideal experimental techniques to evaluate the supercapacitive behavior of any materials.[1, 2] Figure 7a shows the CV curves of N- Graphene recorded at different scan rates ranging from 10 to 200 mVs^{-1} in 1 M H_2SO_4 aqueous solution within a potential window from -0.2 to 0.8 V vs. SCE. The rectangular shapes of voltammograms exhibit a mirror image of the cathodic and anodic parts, indicating ideal capacitor behaviour of pristine and N- Graphene. As the sweep rate increases, the voltammetric current increases, indicating the better rate capability and reversibility. Figure 7b shows the variation of current density with scan rate offer slight line revealing the surface adsorption/desorption process.

The typical galvanostatic charge-discharge curves recorded for N- Graphene are shown in Figure 8 at a current density of 1 $mAcm^{-2}$. The linear variation of potentials with time is another finger print evidence for capacitive behaviour.[1, 2] The highly symmetrical charge-discharge curves indicate the excellent electrochemical reversibility during charge-discharge

process. The specific capacitance of N- Graphene (3 mL ammonium hydroxide) is found to be 459 Fg^{-1} at a current density of 1 $mAcm^{-2}$ which is several times higher than that of the compared RG materials and also much larger than the reported N- Graphene materials.[19, 35, 36] Moreover, the specific capacitance value of N- Graphene obtained in the present method is even comparable to those of metal oxide / graphene and polymer / graphene.[37-41] The super capacitance values for various types of N sources for N doping used in the literature and the reported values are shown in Table 1. Figure 8 shows the variation in specific capacitance as a function of N doping and volume of ammonium hydroxide. Literature indicate that specific capacitance is drastically affected by the amount of N-doping in graphene.[31] But, increasing the amount of ammonium hydroxide will also affect the structure of graphene (RGO) as it is observed from TEM and SAED data (Figure 5).

A drastic drop in the capacitance value was observed when the amount of ammonium hydroxide increased from 3 mL to 5 mL and it may be due to the structural distortion, and also due to the lowering the of the amount of nitrogen to 0.9 atomic % from 4.5 atomic %. But further increase in the amount of ammonia solution increases the amount of nitrogen, and hence, though the structural distortion happened, the amount of nitrogen was increased from 0.9% to 1.7 atomic % when the ammonia solution is increased from 5 mL to 7 mL. Again increase in the ammonia from 7 mL to 10 mL completely amorphized the graphitic backbone and hence though the amount of nitrogen is increased, its capacitance value got decreased. Moreover, out of various nitrogen functionalities, it is reported that pyridinic nitrogen is contributing to the supercapacitance of the resultant doped structure.[35] The capacitance variation follows the same trend as that of the percentage of pyridinic nitrogen (inferred from the XPS measurements) present in the samples. This is also in tune with the earlier reports.[35]

In order to understand the rate capability of N-doped graphene, galvanostatic charge/discharge curves are recorded at different current densities ranging from 1 to 20 $mAcm^{-2}$. Figure 9 shows the specific capacitance of N- Graphene (3 mL) as function of current density. The specific capacitance values of N- Graphene (3 mL) are calculated to be 459, 242, 209, 186 and 186 Fg^{-1}at 1, 2, 5, 10 and 20 $mAcm^{-2}$, respectively. The improved specific capacitance of N- Graphene (3 mL) is well maintained even at higher current densities. For instance, specific capacitance of 186 Fg^{-1} could be retained even at 20 $mAcm^{-2}$ current density indicating that the N-doping does not lead to any deterioration from the original power capability of graphene.[36]

Evaluation of supercapacitors in terms of specific power (SP) and specific energy (SE) is of practical interest. The values of SP and SE were calculated using these below equation respectively,

$$SE = \frac{\frac{It\Delta E}{m}}{2} \qquad 2$$

$$SP = \frac{\frac{I\Delta E}{m}}{2} \qquad 3$$

Where, I is current in amps used for charge/discharge cycling, t is the time revised discharge, m is the mass in grams of the active material and ΔE is the operating potential window in volt of charge or discharge.

Figure 9 inset shows a Ragone plot for the N- Graphene electrodes. It is observed that SE decreases with increasing SP. The SE values are high, being 25.8 – 63.5 W h kg^{-1}, while the SP values are in the range 0.7 – 15.5 kW kg^{-1}.

Hence, in the present investigation on N- Graphene synthesised using ammonium hydroxide solution by hydrothermal method indicates the presence of large amount graphitic

and pyrrolic nitrogen in the graphene sheet (schematic, Figure 6 d). XPS results further suggest that the amount of N doping reached highest for 3 mL ammonium hydroxide treated graphene oxide, and further increase in the ammonium hydroxide did not help to improve the nitrogen content in graphene. But instead, large amount of ammonium hydroxide destabilised the structure of graphene (as it is evident from TEM Figure 5 e-f and XRD results Figure 1), and the amount of nitrogen is also drastically reduced. This is in tune with the earlier reports,[31, 32] those questions the stability of graphene under alkaline treatment. Hence, it has to be concluded that, highest level of N-doping achieved in this method is ~4.5 atomic %, and this contributed to the highest ever reported capacitance value of ~459 Fg^{-1} for nitrogen doped graphene.

Conclusions

A simple and effective route for the synthesis of N- Graphene by a one-step hydrothermal process using ammonium hydroxide as nitrogen source is demonstrated, and achieved 4.5 atomic % of N-doping. $N1_S$ spectrum showed the presence of pyridinic, pyrrolic, graphitic and pyridinic oxide nitrogens' in the doped graphene structure. The improvement in the electrochemical activities *via* doping is studied using supercapacitor measurements, and these studies showed the highest value, 459 Fg^{-1} at 1 mA current density, ever reported for N- Graphene, with excellent cycle stability.

Acknowledgements: M. Praveen Kumar and Deepak K. Pattanayak thank CSIR, India for financial support through MULTIFUN (CSC 0101). Central Instrument Facility (CIF) staff Mr. A. Rathish Kumar (TEM in charge), CSIR-CECRI, Karaikudi for taking TEM images is greatly appreciated.

REFERENCES

1 B. E. Conway, Electrochemical supercapacitors, Scientific fundamentals and technological applications, Kluwer Academic / Plenum publishers, New York **1999**.

2 S. Sarangapani, B. V. Tilak and C. P. Chen, *J. Electrochem. Soc*., 1996, **143**, 3791.

3 F. M. Hassan, V. Chabot, J. Li, B. K. Kim, L. R. Sandoval and A. Yu, *J. Mater. Chem. A*., 2013, **1**, 2904-2912.

4 Y. Zhu, S. Murali, M. D. Stoller, K. J. Ganesh, W. Cai, P. J. Ferreira, A. Pirkle, R. M. Wallace, K. A. Cychosz, M. Thommes, D. Su, E. A. Stach and R. S. Ruoff, *Science*., 2011, **332**, 1537-1541.

5 W. Deng, X. Ji, Q. Chen and C. E. Banks, *RSC Advances.,* 2011, **1**, 1171-1178.

6 G. Zhou, D. W. Wang, F. Li, L. Zhang, N. Li, Z. S. Wu, L. Wen, G. Q. (Max) Lu and H. M. Cheng, *Chem. Mater.,* 2010, **22**, 5306-5313.

7 Z. S. Wu, D. W. Wang, W. Ren, J. Zhao, G. Zhou, F. Li and H. M. Cheng, *Adv. Funct. Mater.,* 2010, **20**, 3595-3602.

8 L. Lai, H. Yung, L. Wang, B. K. Tec, J. Zhong, H. Chou, L. Chen, W. Chen, Z. Shen, R. S. Ruoff and J. Lin, *ACS nano*., 2012, **6**, 5941-5951.

9 H. Gomez, M. K. Ram, F. Alvi, P. Villalba, E. (Lee) Stefanakos and A. Kumar, *J. Power Source*., 2011, **196**, 4102-4108.

10 B. Biel, X. Blase, F. Triozon and S. Roche, *Phys. Rev. Lett.,* 2009, **102**, 096806.

11 S. F. Huang, K. Terakura, T. Ikeda, M. Boero, M. Oshima and J. Miyata, *Phys. Rev. B,* 2009, **80**, 235410.

12 Y. Zheng, Y. Jiao, L. Ge, M. Jaroniec and S. Z. Qiao, Angew. Chem., 2013, **125**, 3192-3198.

13 L. L. Zhang, X. Zhao, H. Ji, M. D. Stoller, L. Lai, S. Murali, S. Mcdonnell, B. Cleveger, R. M. Wallace and R. S. Ruoff, *Energy Environ. Sci*., 2012, **5**, 9618-9625.

14 B. Mortazavi, S. Ahli, V. Toniazzo and Y. Remond, *Phy. Lett. A.,* 2012, **376**, 1146-1153.

15 Y. Xue, B. Wu, L. Jiang, Y. Guo, L. P. Huang, J. Chen, J. Tan, D. Geng, B. Luo, W. Hu,G. Yu and Y. Lui, *JACS*., 2012, **134**, 11060-11063.

16 C. Wang, Y. Zhou, L. He, T. W. Ng, G. Hong, Q. H. Wu, F. Gao, C. S. Lee and W. Zhang, *Nanoscale.,* 2013, **5**, 600-605.

17 X. Wang, X. Li, L. Zhang, Y. Yoon, P. K. Weber, H. Wang, J. Guo and H. Dai1, *Science.,* 2009, **324**, 768.

18 Z. Lin, G. Waller, Y. Liu, M. Liu and C. P. Wong, *Adv. Energy Mater*., 2012, **2**, 884-888.

19 Y. Lu, F. Zhang, T. Zhang, K. Leng, L. Zhang, X. Yang, Y. Ma, Y. Huang, M. Zhang and Y. Chen, *Carbon*, 2013, **63**, 508-516.

20 P. Chen, J. J. Yang, S. S. Li, Z. Wang, T. Y. Xiao, Y. H. Qian and S. H. Yu, *Nano energy*., 2013, **2**, 249-256.

21 Y. Zhao, C. Hu, H. Cheng, G. Shi and L. A. Qu, *Angewandte chemie international edition*., 2012, **51**, 11371-11375.

22 L. Sun, L. Wang, C. Tain, Y. Xie, K. Shi, M. Li and H. Fu, *RSC Advances.,* 2012, **2**, 4498-4506.

23 J. W. Lee, J. M. Ko and J. D. Kim, *ElectrochemActa.,* 2012, **85**, 459-466.

24 D. C. Marcano, D. V. Kosynkin, J. M. Berlin, A. Sinitskii, Z. Sun, A. Slesarev, L. B. Alemany, W. Lu and J. M. Tour, *ACS Nano.,* 2010, **4(8)**, 4806-4814.

25 S. Seo,Y. Yoon, J. Lee, Y. Park and H. Lee, *ACS Nano*., 2013, **7(4)**, 3607-3615.

26 D. Geng, Y. Songlan, Y. Zhang, J. Yang, J. Liu, R. Li, T. K. Sham, X. Sun, S. Ye and S. Knights, *App. Surf. Sci.,* 2011. **257**, 9193-9198.

27 B. X. Fan, W. Peng, Y. Li, X. Li, S. Wang, G. Zhang and F. Zhang, *Adv. Mater.,* 2008, **20**, 4490-4493.

28 B. P. Vinayan, R. Nagar and S. Ramaprabhu, *J. Mater. Chem*., 2012, **22**, 25325-25334.

29 M. A. Pimenta, G. Dresselhaus, M. S. Dresselhaus, L. G. Cancado, A. Jorioa and R. Saitoe, *Phys. Chem. Chem. Phys*., 2007, **9**, 1276-1291.

30. M. Acik, G. Lee, C. Mattevi, A. Pirkle, R. M. Wallace, M. Chhowalla, K. Cho, and Y. Chabal, *J.Phys.Chem.C,* 2011, **115**, 19761-19781.

31 L. Lai, L. Chen, D. Zhan, L. Sun, J. Liu, S. H. Lim, C. K. Poh and Z. Shen, J. Lin, *Carbon,* 2011, **49**, 3250-3257.

32 M. Seredych and T. J. Bandosz, *J. Phys. Chem. C.,* 2007, **111**, 15596-15604.

33 Z. Luo, S. Lim, Z. Tian, J. Shang, L. Lai, B. MacDonald, C. Fu, Z. Shen, T. Yu and J. Lin, *J. Mater. Chem*., 2011, **21**, 8038-8044.

34 L. Lai, J. R. Potts, D. Zhan, L. Wang, C. K. Poh, C. Tang, H. Gong, Z. Shen, J. Lin and R. S. Ruoff, *Energy Environ. Sci*., 2012, **5**, 7936-7942.

35 H. Cao, X. Zhou, Z. Qin and Z. Liu*, Carbon,* 2013, **56**, 218-223.

36 H. M. Jeong, J. W. Lee, W. H. Shin, Y. J. Choi, H. J. Shin, J. K. Kang and J. W. Choi, *Nano Lett*., 2011, **11**, 2472-2477.

37 H. Wang, Q. Hao, X. Yang, L. Lu and X. Wang, *Electrochem. Com.,* 2009, **11**, 1158-1161.

38 J. Xu, K. Wang, S. Z. Zu, B. H. Han and Z. Wei, *ACS Nano*., 2010, **4**, 5019-5026.

39 Q. Wu, Y. Xu, Z. Yao, A. Liu and G. Shi, *ACS Nano.,* 2010, **4**, 1963-1970.

40 Y. Munaiah,Y.; B. G. S. Raj, T. Prem Kumar and P. Ragupathy, *J. Mater. Chem*. A., 2013, **1**, 4300-4306.

41 M. Ashokkumar, T. N. Narayanan, A. L. Mohana Reddy, B. K. Gupta, B. Chandrasekaran, S. Talapatra, P. M. Ajayan and P. Thanikaivelan, *Green Chem.,* 2012, **14**, 1689-1695.

42 C. Wang, Y. Zhou, L. Sun, Q Zhao, X. Zhang, P. Wan and J. Qiu, *Phys. Chem.,* 2013, **117**, 14912-14919.

43 P. Wang, H. He, X. Xu and Y. Jin, *App. Mater. Interface*., 2014, **6**, 1563-1568.

44 Z. Wen, X. Wang, S. Mao, Z. Bo, H. Kim, S. Cui, G. Lu and X. Feng, J. Chen, *Adv. Mater.* 2012, **24**, 5610-5616.

FIGURE CAPTIONS

Figure 1. XRD pattern of (a) Graphite powder (b) GO (c) Graphene, (d) - (g) N-doped graphene prepared from GO and 3, 5, 7 and 10 mLof ammonium hydroxide ,respectively by hydrothermal method.

Figure 2. Raman spectrum of (a) Graphite powder (b) GO (c) Graphene, (d) - (g) N-doped graphene prepared from GO and 3, 5, 7 and 10 mL of ammonium hydroxide, respectively by hydrothermal method. I_D / I_G ratio for GO, graphene and N-doped graphene are also shown.

Figure 3. FT-IR spectra of (a) GO (b) Graphene, (c) - (f) N-doped graphene prepared from GO and 3, 5, 7 and 10 mL of ammonium hydroxide, respectively by hydrothermal method.

Figure 4. FE-SEM images of (a) Graphite powder, (b) Graphene and (c) - (f) N-doped graphene prepared from GO and3, 5, 7 and 10 mL of ammonium hydroxide, respectively by hydrothermal method.

Figure 5. TEM images of (a) Graphite powder (b) Graphene, and (c) - (f) N-doped graphene prepared from GO and 3, 5, 7 and 10 mL of ammonium hydroxide respectively by hydrothermal method and their corresponding SAED pattern.

Figure 6. XPS spectrum of N-doped graphene prepared from GO using 3 mL ammonium hydroxide (a) full scale serve pattern and high resolution spectrum of (i) carbon (ii) nitrogen (iii) oxygen and (iv) all types of nitrogen in a graphene lattice as an inset. High resolution XPS spectrum for (b) 7 mL (c) 10 mL and (d) one sheet visualization of all types of nitrogen.

Figure 7. (a) CV curves of the N-doped graphene electrode in 1M H_2SO_4 with different scan rates 10, 20, 40, 80, 100 and 200 $mVs^{-1}$and (b) the relationship between current vs scan rate of N- doped graphene.

Figure 8. Achieved specific capacitance vs. volume of ammonium hydroxide. (The amount of N content is indicated in the figure). Galvanostatic charge/discharge curves of N-doped graphene (3mL ammonia solution) electrode at a current density of 1 $mAcm^{-2}$ in 1 M H_2SO_4 is shown as inset.

Figure 9. Specific capacitance vs current density and Ragone plot for N- doped graphene prepared from 3 mL of ammonium hydroxide solution is shown as inset.

TABLE CAPTIONS

Table 1. Literature reports on amount of N-doping, synthesis method and specific capacitance value.

Table 2. Amount of N- content (at %) as calculated from XPS and p^H of different amount of ammonium hydroxide solution used to prepare N-doped graphene.

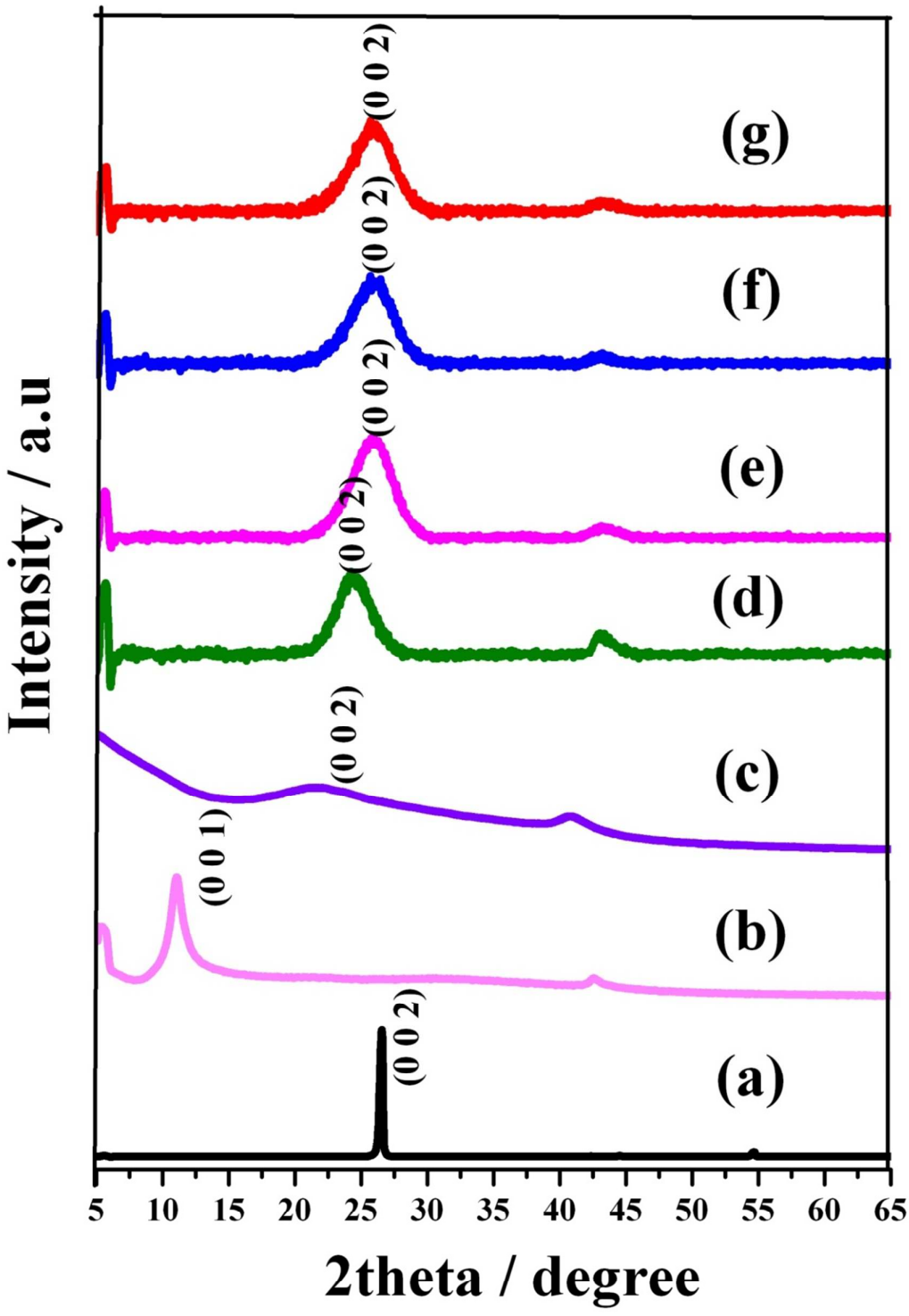

Figure 1:

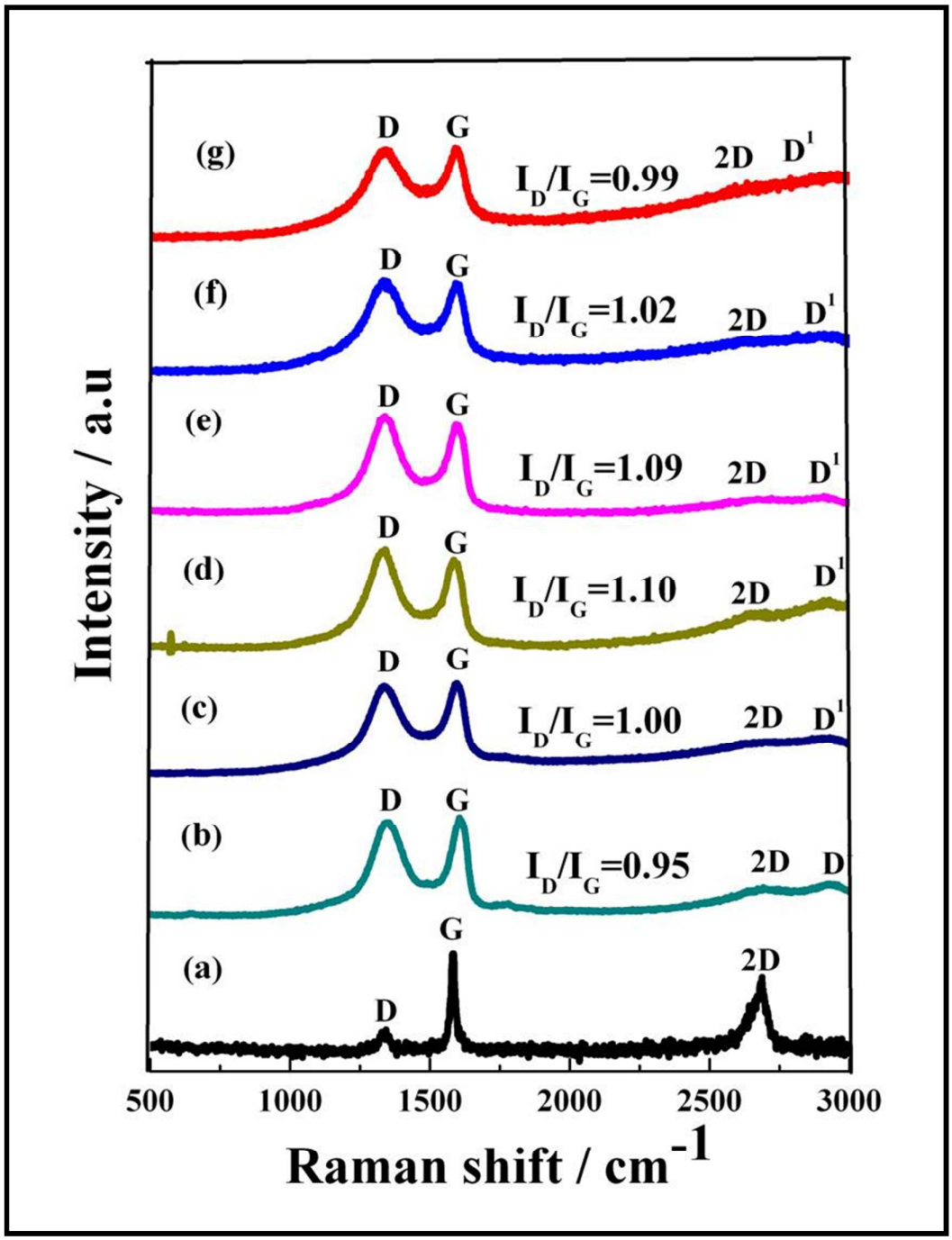

Figure 2:

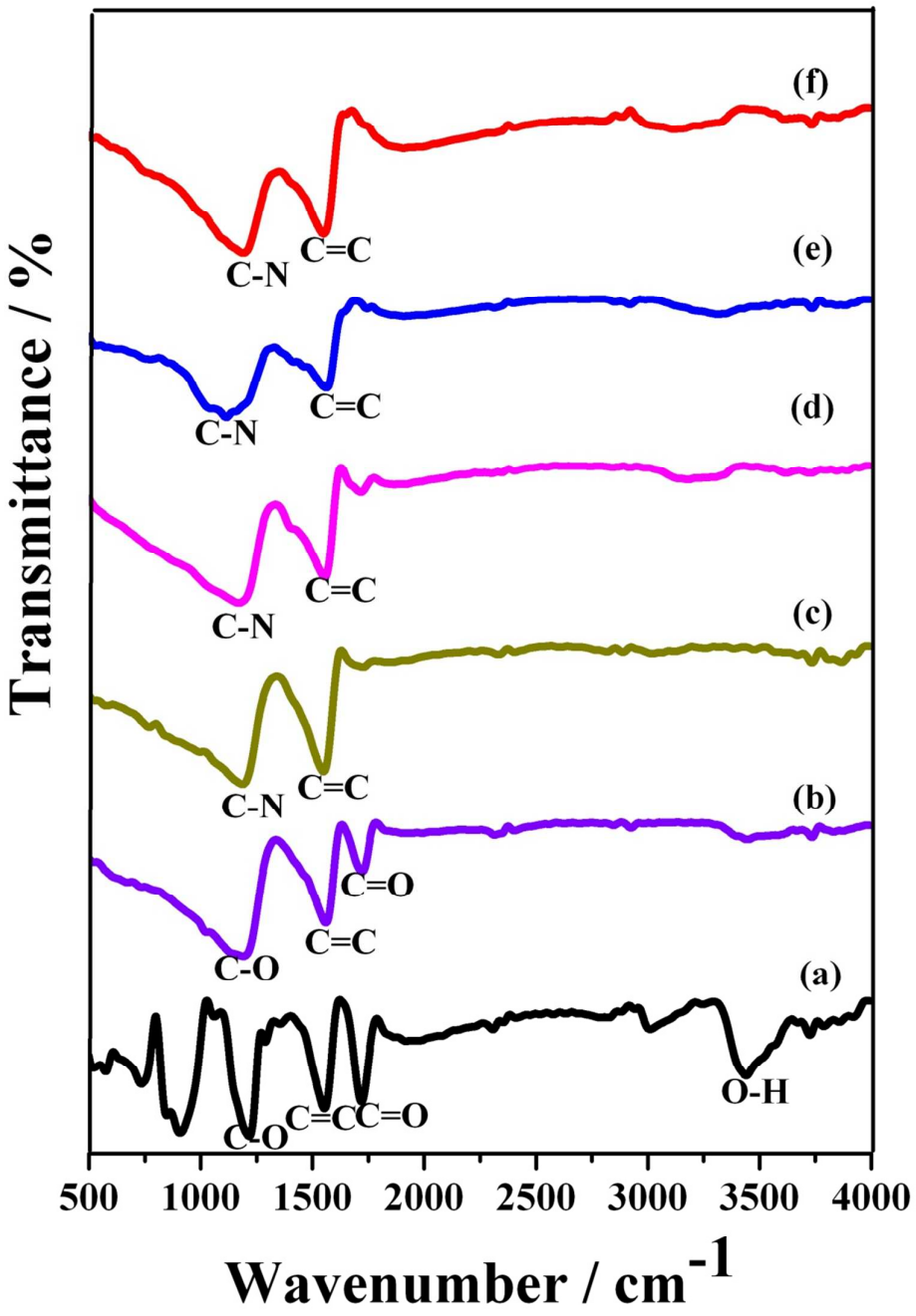

Figure 3:

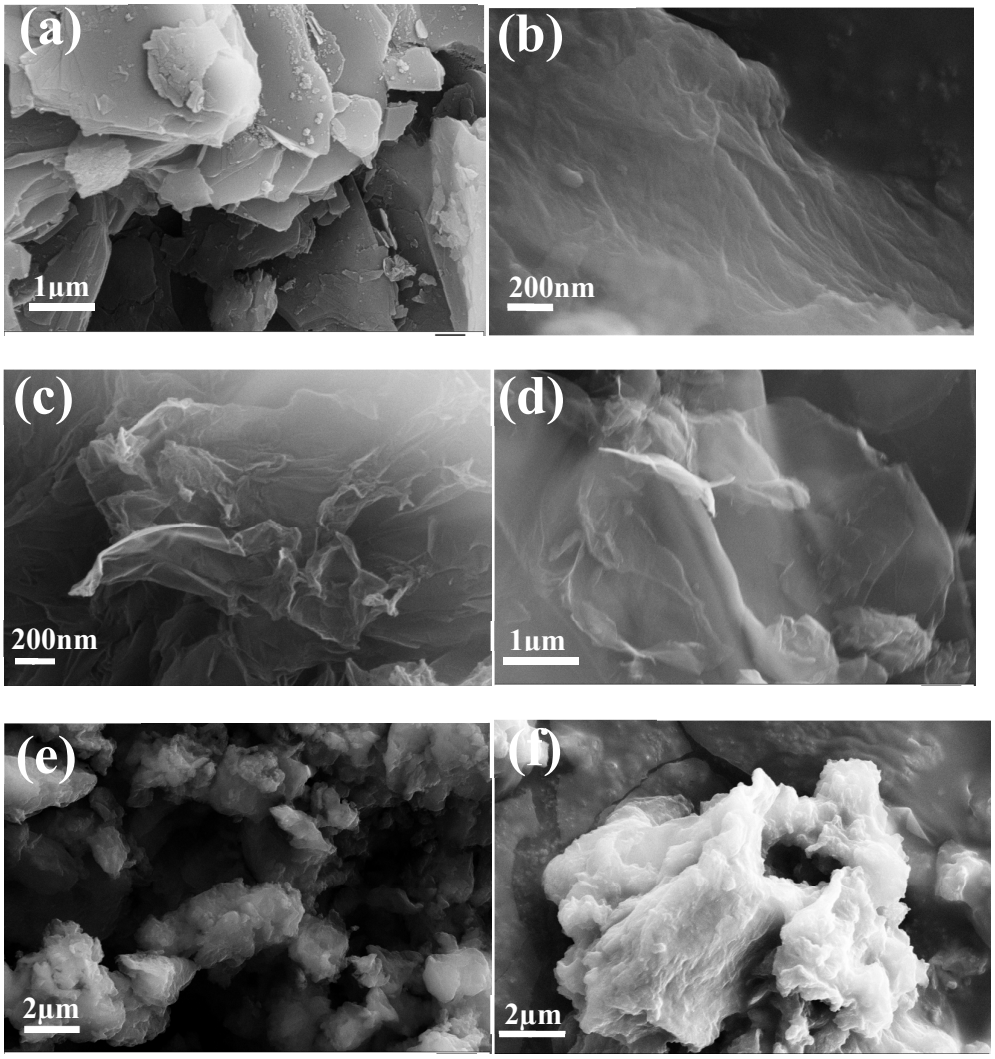

Figure 4:

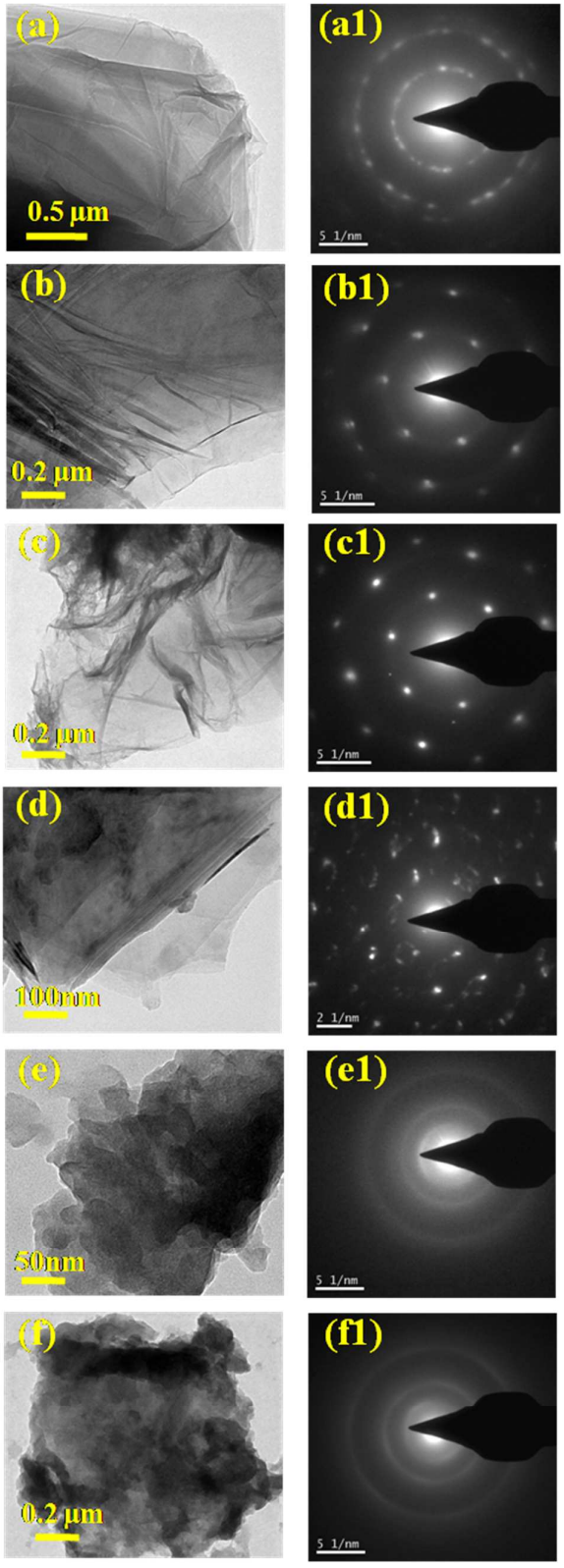

Figure 5:

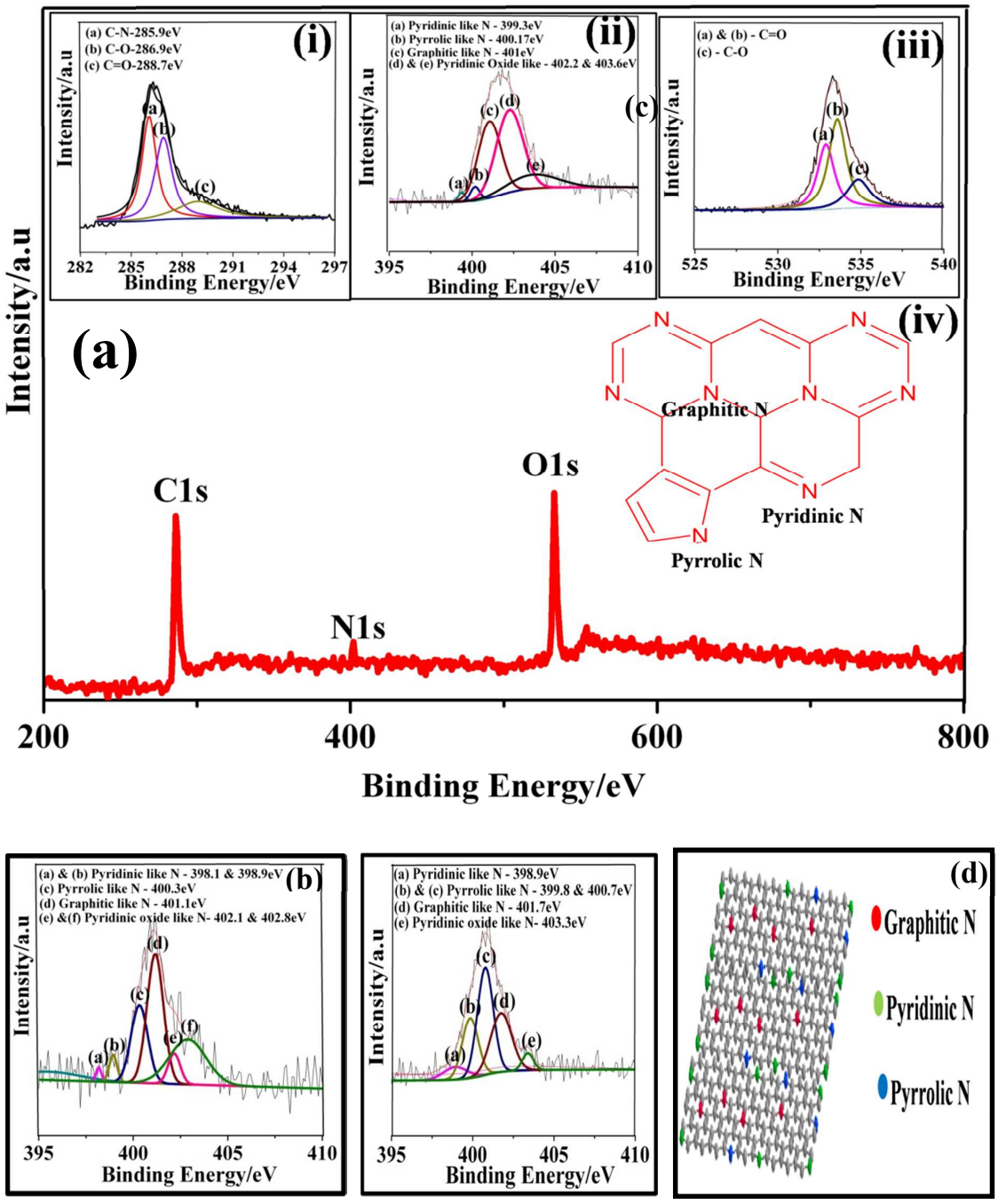

Figure 6:

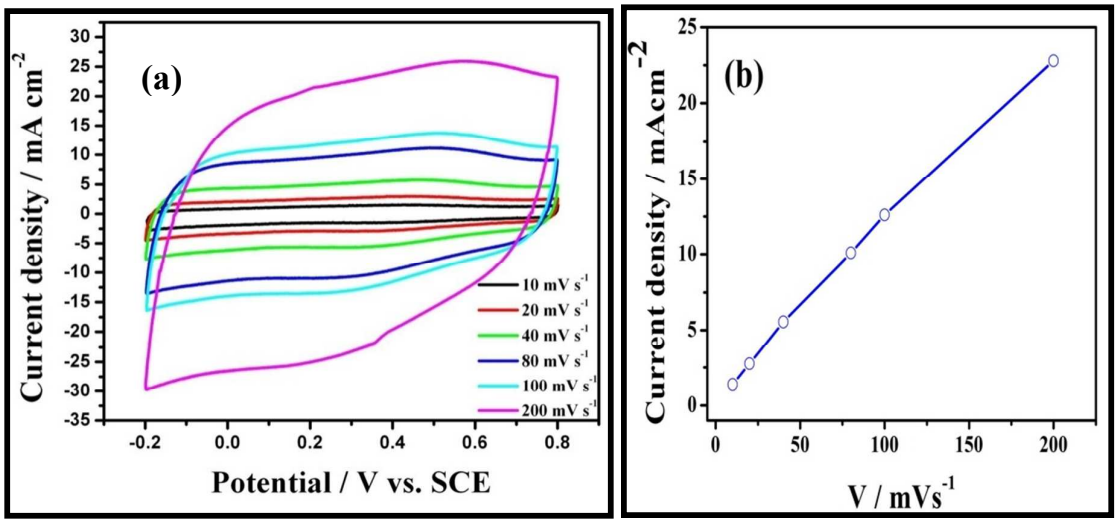

Figure 7:

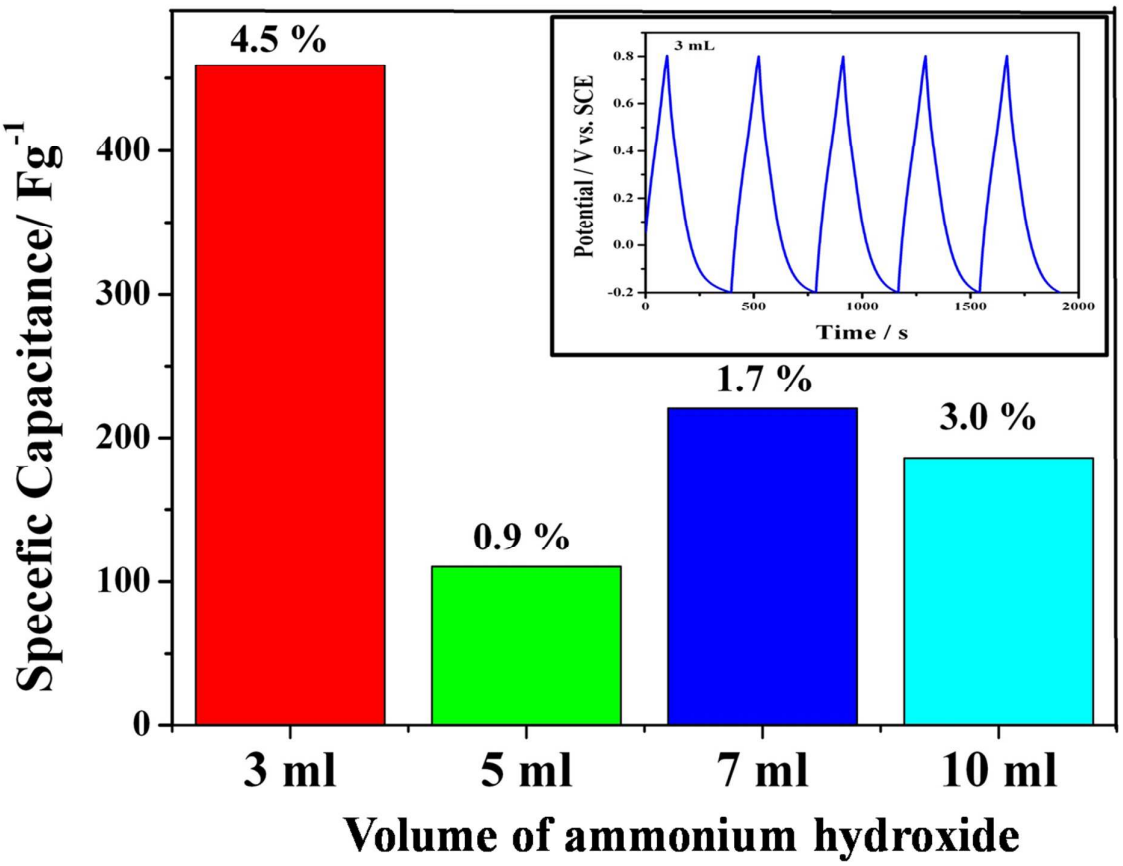

Figure 8:

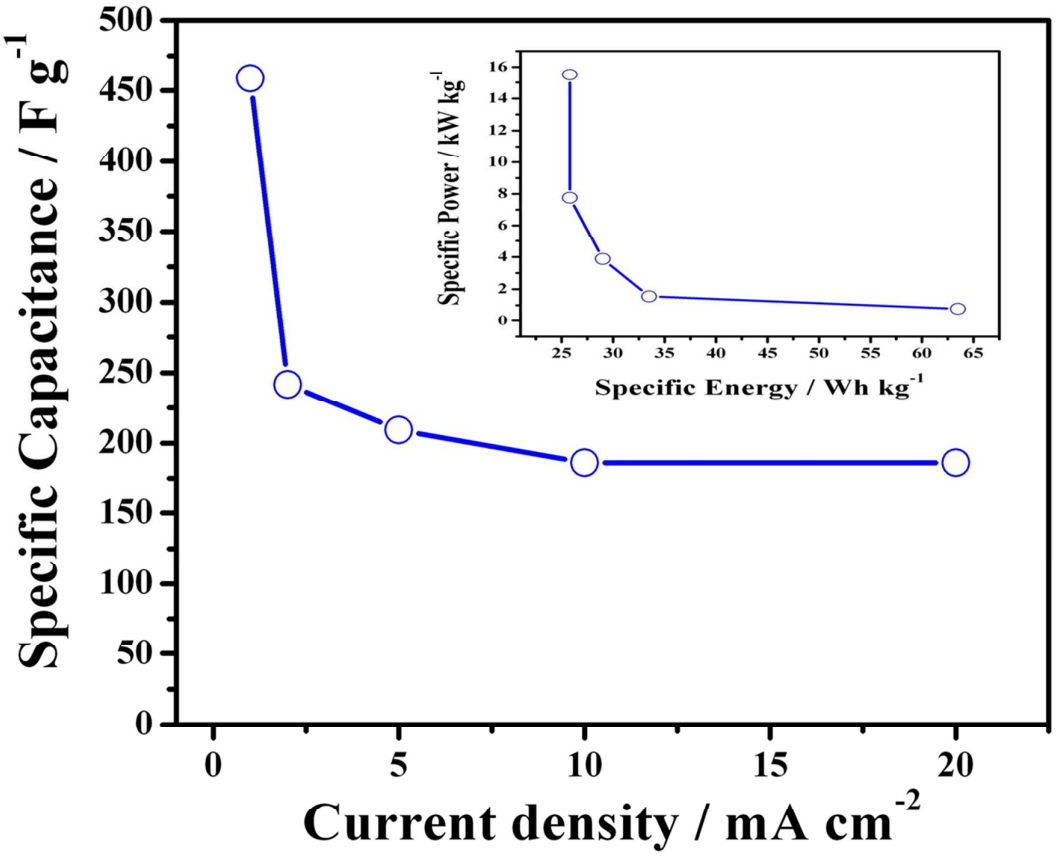

Figure 9:

Table 1

S. No	Atomic percentage(%)	Synthesis method	Capacitance(Fg^{-1})	Reference
1.	7.7	solvothermal method	301	19
2.	8.62	hydrothermal method	161	23
3.	12.75	solvothermal method	170	36
4.	2.51	plasma process	280	34
5.	2.77	hydrothermal method	194	3
6.	3.2	thermally exfoliated	82	42
7.	5.96	chemical method	244	43
8.	9.6	thermally exfoliation process	248	44

Table 2

S. No	NH_4OH amount	Atomic percentage (%)	p^H value
1	3 mL	4.5	11
2	5 mL	0.9	11.30
3	7 mL	1.7	12
4	10 mL	3.0	12.30

Scheme: Large level of N-doped graphene prepared by facile route with high supercapacitance.